Supporting Information

Jogler et al. 10.1073/pnas.1012694108

SI Materials and Methods.

Electron Microscopy. For chemical fixation, cells were incubated in 2.5% glutardialdehyde containing fixative buffer (75 mM sodium cacodylate, 2 mM $MgCl_2$, pH 7.0), for 1 h at room temperature. Afterward, samples were rinsed several times in fixative buffer and postfixed at room temperature for 1 h with 1% osmium tetroxide in fixative buffer. After two washing steps in water, the cells were stained *en bloc* for 30 min with 1% uranyl acetate in 20% acetone. Dehydration was performed with a graded acetone series. Samples were then infiltrated and embedded in Spurr's low-viscosity resin.

For high-pressure freezing, aluminum platlets were filled with concentrated cell suspensions and the cells immobilized by high-pressure freezing (Leica; HPM100). Freeze substitution was performed in acetone with 2% osmium tetroxide and 0.2% uranyl acetate, including 5% water. After embedding the samples in Epon, ultrathin sections were cut with a diamond knife and mounted onto uncoated copper grids. The sections were post-stained with aqueous lead citrate (100 mM, pH 13.0).

Transmission electron micrographs were taken with an EM 912 electron microscope (Zeiss) equipped with an integrated OMEGA energy filter operated at 80 kV in the zero loss mode. The FIB serial sectioning was performed by a Zeiss-Auriga workstation. The focused ion beam consisted of Ga^+ ions accelerated by a voltage of 30 kV. In the cut-and-view mode, sections ranging in thickness between 5 nm and 10 nm (dependent on the magnification) were produced with the FIB and FESEM images, which were recorded at 1.5 kV using the in-lens energy selective backscattered (EsB) detector. Specimens were tilted to an angle of 54°; images were tilt corrected for undistorted surface view.

For SEM, drops of the sample were placed onto a glass slide, covered with a coverslip, and rapidly frozen with liquid nitrogen. The coverslip was removed with a razor blade and the glass slide was immediately fixed with 2.5% glutaraldehyde in 75 mM cacodylate buffer (pH 7.0), postfixed with 1% osmium tetroxide in fixative buffer, dehydrated in a graded series of acetone solutions, and critical-point dried after transfer to liquid CO_2. Specimens were mounted on stubs, coated with 3 nm platinum using a magnetron sputter coater, and examined with a Zeiss Auriga scanning electron microscope operated at 1–2 kV. For cryo-scanning electron microscopy high-pressure frozen samples were fractured with a Leica EM MED020, sublimated for 1–2 min a −95 °C and coated with 3 nm of tungsten, transferred to the scanning electron microscope and examined at 1 kV.

Single Cell Sorting and Whole Genome Amplification (WGA). Single cell sorting was achieved via an Eppendorf TransferMan NK2 micromanipulator and the Eppendorf CellTram Oil manual hydraulic pressure-control system mounted to an Olympus BX61 microscope equipped with a 40× LD objective and a double slide holder. Samples were kept on microscopic slides attached to a custom-build plastic frame, while an Advalytix AmpliGrid AG480F was placed next to it in the double slide holder (Fig. S6*C*). Five to 15 individual Mbav cells were transferred via micromanipulation from the 5-μL sample droplet (containing variable amounts of MTB) into two different washing droplets (5 μL) and finally into 0.75 μL sample buffer (Illustra GenomiPhi V2 DNA amplification kit; GE Healthcare) covered with 5 μL of sealing solution (Advalytix). Together, this washing procedure resulted in a 10^{18}-fold dilution of sample liquid, which is likely to have outdiluted any contaminating DNA to extinction (Fig. S10). Loaded AmpliGrid was transferred into a customized AmpliSpeed slide cycler (Advalytix) calibrated to operate at 4 °C. Samples were heated to 95 °C for 3 min and incubated at 4 °C for 10 min. A total of 0.75 μL of reaction buffer containing enzyme mix (Illustra GenomiPhi V2 DNA amplification kit; GE Healthcare) was added by pipetting on top of the sealing solution (Advalytix) and reactions were incubated for 4 h at 30 °C. The phi29 enzyme was inactivated by incubating the sample at 65 °C for 10 min. After amplification, seven independent reactions—based on a total number of 158 individually sorted Mbav cells—were pooled to overcome phi29 bias and a 16S rRNA gene library was constructed as described previously (1). Sequence analysis of 25 clones revealed identical Mbav sequences (cutoff 99%).

Screening of Fosmid Libraries. Six fosmid libraries that were constructed before were screened via endsequencing as previously described (2, 3). Based on sequence analysis of individually sorted cells after WGA, the primers CJ272 (cactacgccacccttgaagt) and CJ273 (tgaggtaatcggcatcaaca) targeting a 130-bp region of *mamE*, as well as the primers CJ280 (ttgatattacatgacatctg) and CJ281 (cgaggcaacggagaagatac) targeting a 555-bp region of *mamP* were deduced. The PCR-based fosmid library screening was performed as previously described (3).

1. Lin W, Pan Y (2009) Uncultivated magnetotactic cocci from yuandadu park in beijing, china. *Appl Environ Microbiol* 75:4046–4052.
2. Jogler C, et al. (2009) Toward cloning of the magnetotactic metagenome: Identification of magnetosome island gene clusters in uncultivated magnetotactic bacteria from different aquatic sediments. *Appl Environ Microbiol* 75:3972–3979.
3. Jogler C, et al. (2010) Cultivation-independent characterization of 'Candidatus Magnetobacterium bavaricum' via ultrastructural, geochemical, ecological and metagenomic methods. *Environ Microbiol* 12:2466–2478.
4. Preusting H, Kingma J, Huisman G, Steinbüchel A, Witholt B (1993) Formation of polyester blends by a recombinant strain of Pseudomonas oleovorans: Different poly (3-hydroxyalkanoates) are stored in separate granules. *J Environ Polym Degrad* 1: 11–21.

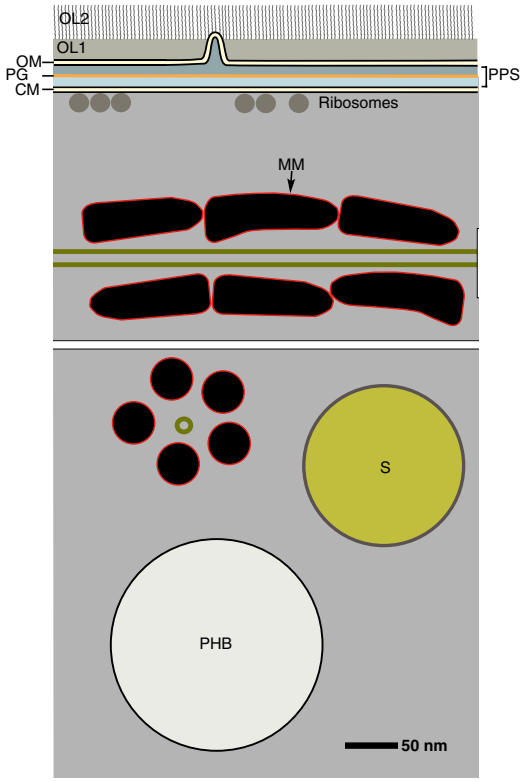

Fig. S1. Schematic representation of the envelop and interior of *Candidatus* Magnetobacterium bavaricum (Mbav) cells according to data shown in Figs. 1–3. The cells have a Gram-negative envelope, which, however, exhibits additional exterior envelope layers. The cytoplasmic membrane (CM), which was frequently found associated with ribosomes, is adjacent to an unusually large (25 to more than 30 nm) periplasmic space (PPS) that is divided by a putative peptidoglycan (PG) layer into a darker outer part and an inner part with lower electron density (Fig. 1 *B*, *C*, and *F*). The outer membrane (OM) is followed by a bipartite outer layer (OL), which is variable in thickness within the range of 45–70 nm (Fig. 1*B*). Its inner part appears homogeneous (Fig. 1*C*, OL1), whereas the outer part frequently displayed brush-like protrusions (OL2, Figs. 1*C* and 2 *D* and *E*). Depending on the particular fixation and imaging technique, dimensions and appearance of this layer were most variable, with optimal visibility obtained by freeze substition. By its low contrast and fuzzy appearance, the OL resembles capsular structures consisting of polysaccharides in other bacteria. Typically, the outer part of the periplasmic space forms numerous ridges, papillae, or "star-like" extensions, which protrude by 20–40 nm into the OL (Fig. 1 *D* and *F*). The extension of the ridges forms a network, which could best be seen in tangential focused ion beam (FIB) sections as dark regions due to the higher electron density of the outer part of the periplasmic space (Fig. 1*E*). These ridges became more obvious after conventional fixation due to shrinkage of the cells both in TEM and SEM (Fig. 1 *F* and *G*). Bullet-shaped magnetite crystals (black), which are each enveloped by a magnetosome membrane (MM), are aligned in three to six (mostly five) strands, which are arranged around a tubular cytoskeletal structure (green) to form a regular rosette-like magnetosome bundle. In addition to magnetosomes, sulfur globuli (S) and polyhydroxybutyrate-like (PHB) granules are present within the cytoplasm (Fig. 1*B* and Fig. S2).

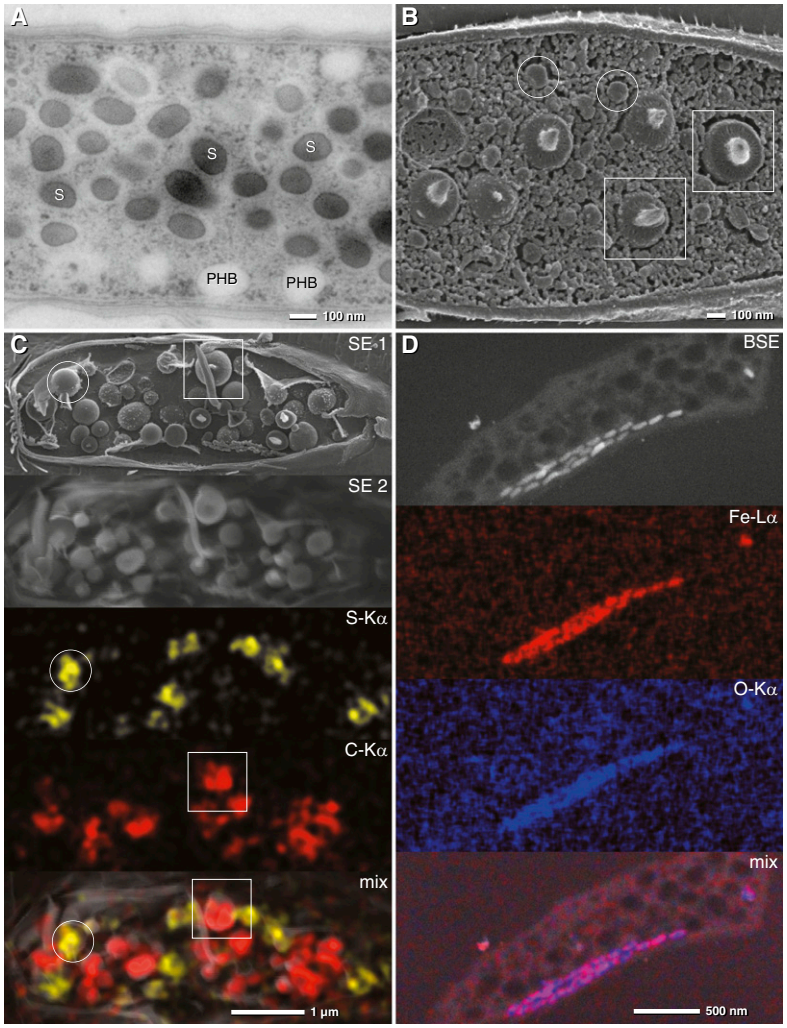

Fig. S2. TEM, SEM, and X-ray analysis of the different intracellular inclusions. (*A*) TEM of a section from high-pressure frozen and freeze-substituted *Candidatus* Magnetobacterium bavaricum (Mbav) cell. Two types of roughly globular inclusions are visible: electron dense sulfur globules (50–150 nm) and electron translucent polyhydroxybutyrate (PHB) granules (300–500 nm). The PHB granules can be recognized by their characteristic freeze-fracturing behavior resulting in the formation of "mushroom"-like protrusions (squares) (*4*) as seen in cryo-SEM (*B*). Frozen hydrated cell (*C*) before element mapping (SE1) and after mapping (SE2) revealing some distortion by beam damage at the rather high voltage of 4 kV necessary for elemental analysis. Sulfur globules (circles) and PHB granules (squares) can be discerned by their different signals (S-K_a) and higher carbon content of PHB as shown in the *Lower* panels. (*D*) SEM of ultrathin sections of Mbav. Detection of backscattered electron gives a bright signal of the magnetosome crystals (*D*, BSE). X-ray mapping of oxygen and iron generated by the particles is consistent with magnetite (Fe_3O_4).

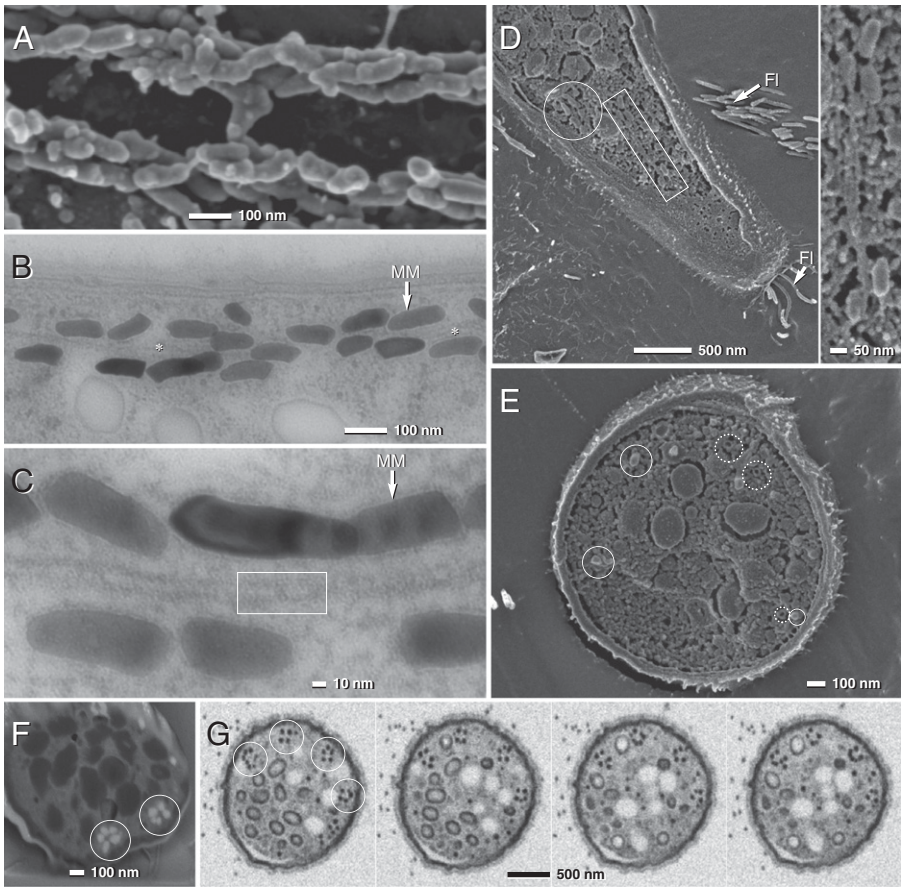

Fig. S3. TEM and SEM micrographs of Mbav magnetosome chains. (*A*) SEM microcraph of a cryofractured cell (after chemical fixation) showing two bundles of magnetosome strands. (*B* and *C*) TEM ultrathin sections of high-pressure frozen and freeze-substituted cells showing strands of magnetosomes aligned parallel to a tubular filamentous structure (asterisk, framed area; MM, magnetosome membrane). (*D* and *E*) Cryo-SEM (frozen hydrated) of tangential (*D*) and cross-fractured (*E*) cells of Mbav (rectangular frame, magnetosomes aligned along MF; solid circles, magnetosomes crystals; dotted circle, empty MM vesicles). (*F* and *G*) SEM of focused ion beam (FIB) sections (*F*), and high-pressure frozen and freeze-substituted (*G*) Mbav cells. Circles indicate several rosette-like magnetosome bundles. Different micrographs in *G* represent selected sections from FIB-milling series (every 10th section is shown from left to right). Each section has a thickness of 8 nm.

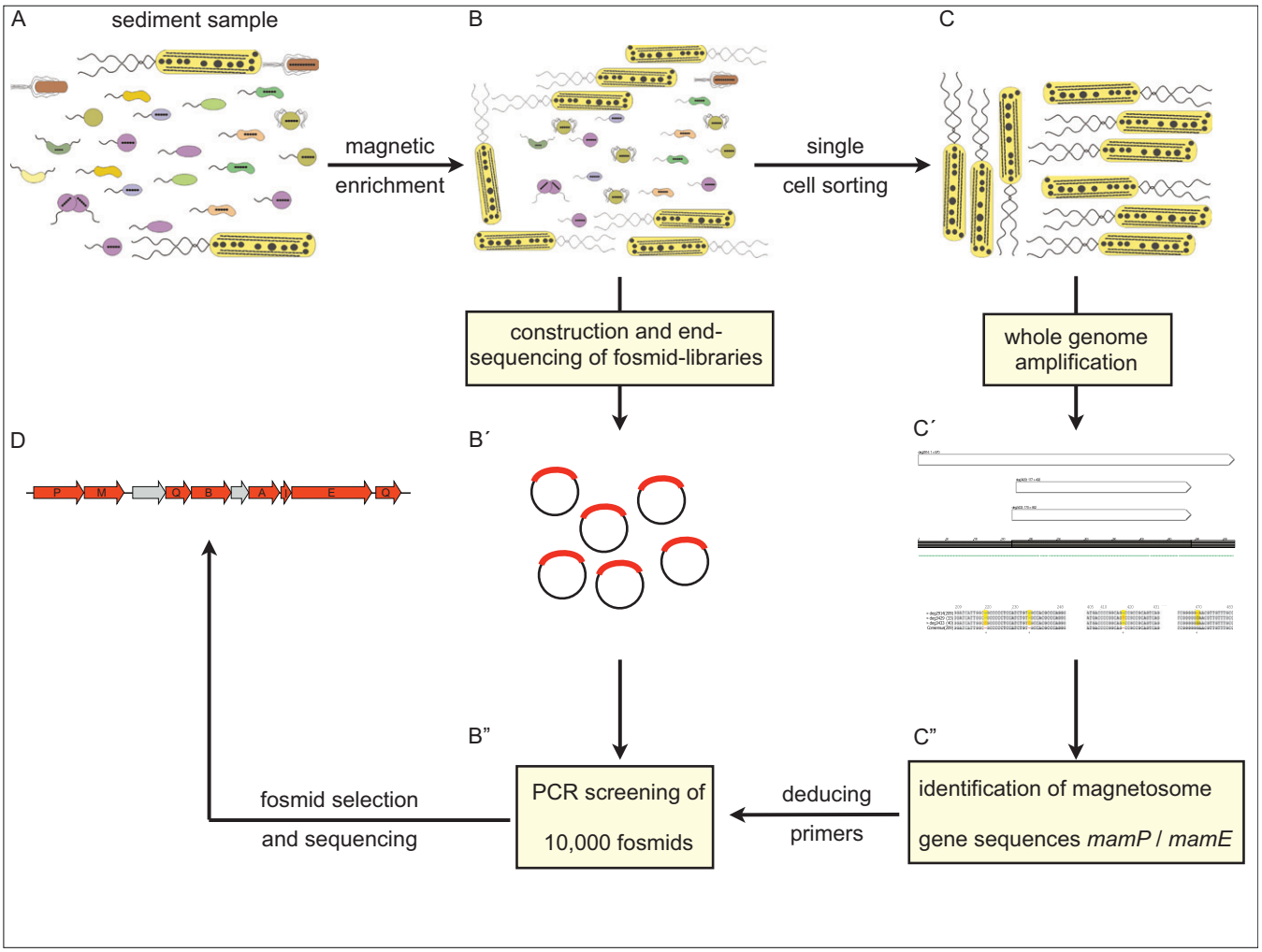

Fig. S4. Schematic representation of the strategy that lead to the identification of a 37-kb genomic fragment of *Candidatus* Magnetobacterium bavaricum (Mbav) containing a part of a putative magnetosome island (MAI). (*A*) Starting point were environmental sediment samples. (*B*) A two-step magnetic separation process resulted in selective collection of MTB highly enriched in Mbav content. (*B′*) This enrichment was used for the construction of metagenomic fosmid libraries and for single cell sorting. (*C*) Single cell sorting via micromanipulation. (*C′*) The manually sorted Mbav cells were subject to phi29 mediated whole genome amplification and subsequent sequence determination via pyrosequencing. (*C″*) Two putative magnetosome gene fragments (*mamE* and *mamP*) were identified. These fragments were used to deduce specific PCR primers. (*B″*) Subsequent screening of fosmid libraries led to the identification of five fosmids. (*D*) Sequence analysis of theses five fosmids resulted in a 37-kb contig containing several magnetosome genes. (*B′*) Conventional endsequencing of the fosmid libraries done in parallel failed to identify any magnetosome gene containing fosmid.

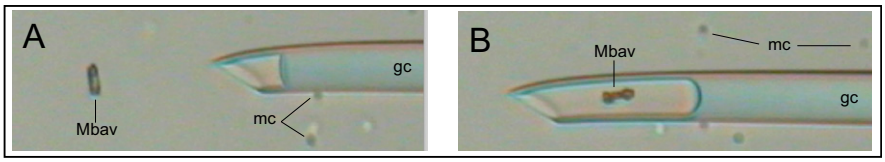

Fig. S5. Micromanipulation of individual Mbav cells from a magnetically enriched mixture of different MTB. Micrographs (400× magnification) show a glass capillary (gc) before *A* and after *B* aspiration of an individual target cell. Contaminating magnetic cocci (mc) can be clearly discriminated.

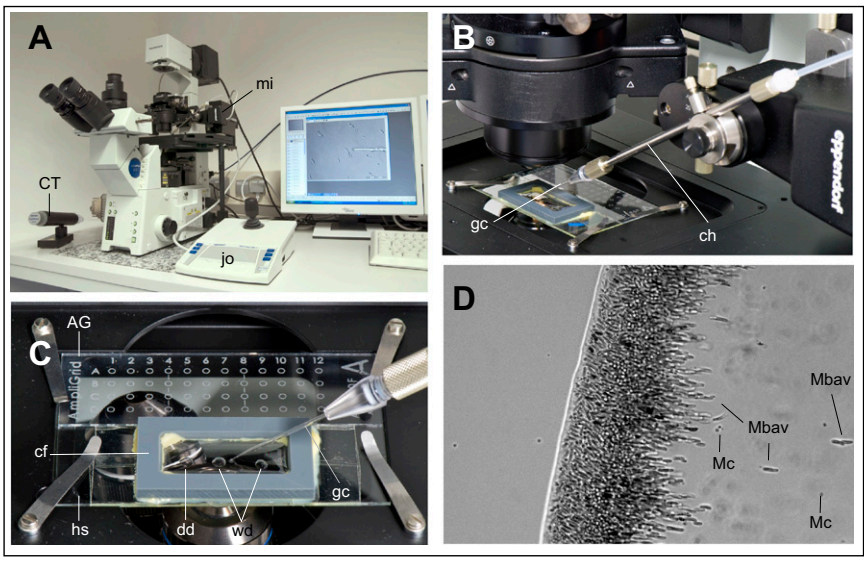

Fig. S6. Experimental setup for single cell sorting for whole genome amplification. (*A*) Eppendorf TransferMan NK2 micromanipulator (mi) attached to an Olympus BX61 microscope equipped with a long distance 40× lens. The micromanipulator is operated by a joystick control unit (jo), whereas aspiration and dispensing of individual cells is achieved by the Eppendorf manual CellTram (CT) hydraulic pressure-control system. (*B*) Capillary holder (ch) equipped with a glass capillary (gc). (*C*) Harvesting slide (hs) and AmpliGrip slide (AG). A custom-made frame (cf) filled with mineral oil prevents evaporation of the donor droplet (dd) and the wash droplets (wd). The glass capillary (gc) is first inserted into the donor droplet (dd), which contains a mixture of magnetically collected MTB from environmental sediment samples. (*D*) Micrograph of a section from a "hanging drop" containing diverse MTB from such an enrichment. *Candidatus* Magnetobacterium bavaricum (Mbav) cells and contaminating magnetotactic cocci (Mc) can be easily distinguished.

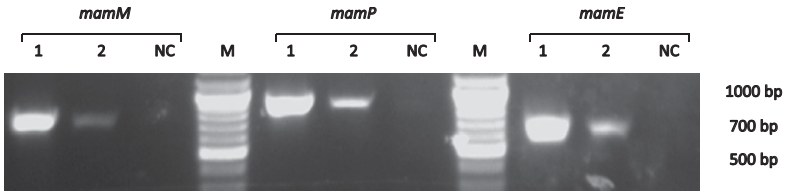

Fig. S7. Results of a control PCR to verify the Mbav origin of representative genes from the 37-kb contig. DNA generated from two independent WGA reactions on one and four individually sorted Mbav cells, respectively, were used as template in two independent PCR experiments (no.1 and no. 2) with primers targeting the *mamM*, *mamP*, and *mamE* genes of Mbav. Bands with a size of 693 bp, 809 bp, and 565 bp, respectively, were amplified as expected (NC, negative control with filter sterilized sample water). As a further control, a 1,068-bp fragment of the Mbav16S rRNA gene was amplified from the same templates using universal primers. Sequence analysis revealed a 100% match to the known 16S rRNA gene sequence of Mbav.

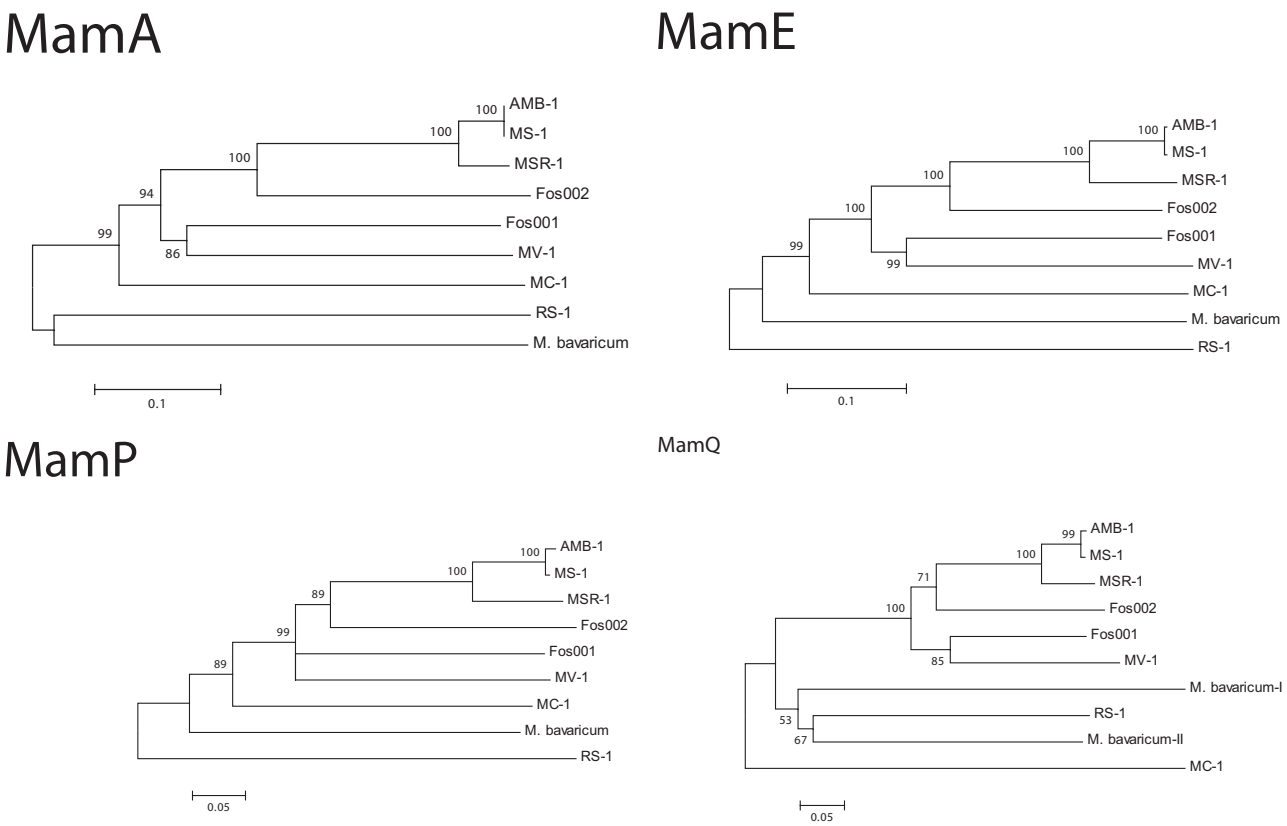

Fig. S8. Phylogenetic trees of further putative magnetosome proteins MamA, -E, -P, -Q, which display branching patterns congruent to those obtained for MamB and MamM. AMB-1, *Magnetospirillum magneticum*; MS-1, *Magnetospirillum magnetotacticum*; MSR-1, *Magnetospirillum gryphiswaldense*; Fos, Metagenomic clone; MV-1, magnetotactic vibrio strain MV-1; MC-1, magnetotactic coccus strain MC-1; and RS-1, *Desulfovibrio magneticus*.

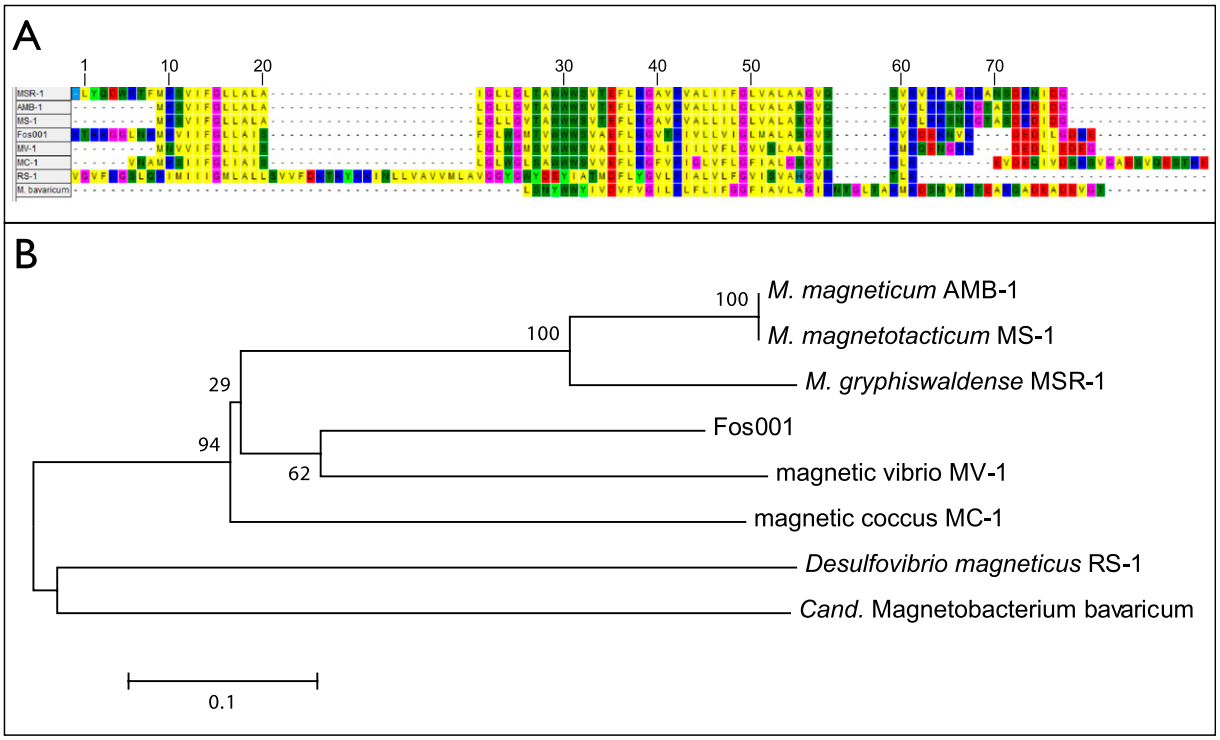

Fig. S9. (*A*) Multiple sequence alignment of MamI homologs from *Candidatus* Magnetobacterium bavaricum (Mbav), selected cultivated MTB, and a metagenomic clone (Fos001). Amino acid positions correspond to the MamI protein of *M. gryphiswaldense* MSR-1. The putative Mbav MamI protein is shorter than all other MamI proteins. (*B*) Phylogenetic tree calculated from the alignment shown in *A*. MamI homologs from *Desulfovibriomagneticus* RS-1 and Mbav cluster together, but are separated from other MTB. Bootstrap values and the bootstrap consensus tree are shown.

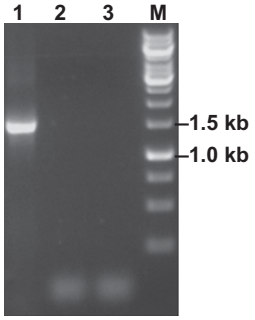

Fig. S10. Results of a nontemplate control experiment for whole genome amplification (WGA).The control experiment was performed as the previously described sorting experiment and the preparation of WGA DNA for pyrosequencing (Fig. S5 and *Materials and Methods*), except one modification: About 15 *Candidatus* Magnetobacterium bavaricum (Mbav) cells were transferred from a 5-μL sample droplet into a 5-μL sorting droplet, which consists of 5 μL of filter-sterilized (0.45 μm pore size) sample water (identical to the 5-μL sample droplet, but without cells). As previously described, sorted cells were subsequently transferred into a 5-μL H_2O droplet for further washing before transfer onto the Ampligrid was performed. After processing 82 cells in total, the capillary was used to harvest nontemplate control samples from sorting- and washing droplet. Together with the sorted cells, these samples were subjected to WGA and subsequent PCR experiments to check for extracellular DNA contaminations. PCR amplification of the 16S rRNA gene from the MTB sample (line 1), the filter-sterilized sample water (line 2), and the H_2O washing droplet (line 3) was performed as previously described (2), (lane M, Fermentas 1-kb DNA ladder). Only lane 1 shows the expected band corresponding to the full-length 16S rRNA gene, whereas lanes 2 and 3 do not show any band. Therefore, it can be confidently concluded from the nontemplate WGA control that the washing procedure was sufficiently stringent to remove any extracellular DNA contaminations.

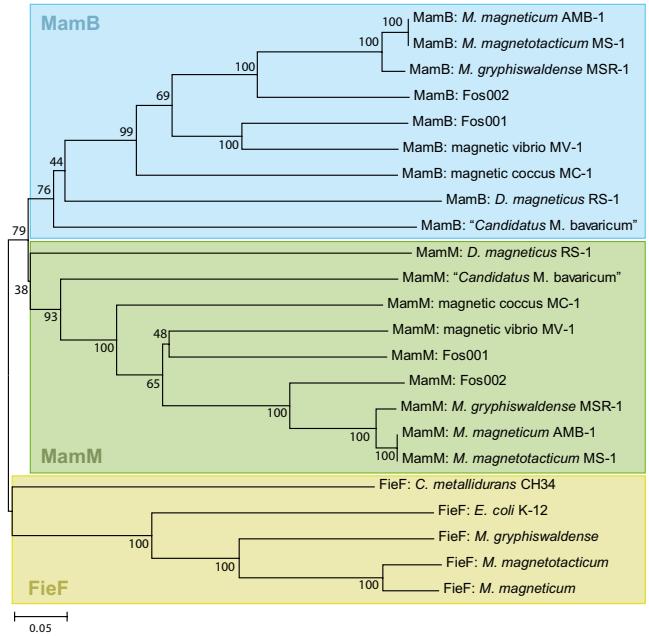

Fig. S11. Phylogenetic tree of cation diffusion facilitator (CDF) proteins of MTB. Two different types of FieF proteins from *Escherichia coli* K12 and *Wautersia metallidurans* served as outgroup and cluster together with FieF proteins from *Magnetospirillum* species (yellow). In contrast, the magnetosome proteins MamB and MamM form separate clusters (blue and green). The predicted MamB and MamM proteins of Mbav branching within these two clusters point toward horizontal gene transfer of *mamM* and *mamB* genes.

Table S1. Blast analysis of proteins encoded by predicted genes against the NCBI database

Locus tag	Annotation	Best hit	Identity, %	*e*-value	aa
emg00001	Hypothetical protein	*Gloeobacter violaceus*	38	1–32	516
emg00002	XRE family transcriptional regulator	*Yersinia pseudotuberculosis*	33	7–17	206
emg00003	Aspartate 1-decarboxylase	*Thermodesulfovibrio yellowstonii*	52	4–32	117
emg00004	4-hydroxy-3-methylbut-2-en-1-yl diphosphate synthase	*Thermodesulfovibrio yellowstonii*	60	3–120	348
emg00005	Hypothetical protein	*Thermodesulfovibrio yellowstonii*	45	3–72	319
emg00006	Hypothetical protein	*Thermodesulfovibrio yellowstonii*	61	1–51	180
emg00007	Transcriptional regulator, MerR family	*Sphaerobacter thermophilus*	33	4–16	128
emg00008	IS1 transposase B	*Escherichia coli*	100	1–94	167
emg00009	Hypothetical protein	*Syntrophomonas wolfei*	30	4–57	791
emg00010	Transposase	Plasmid R100	100	0.0	402
emg00011	Hypothetical protein	*Syntrophobacter fumaroxidans*	41	1–67	1,038
emg00012	Hypothetical protein	*Chloroflexus aggregans*	32	5–64	1,135
emg00013	**Polysaccharide biosynthesis protein**	***Methanococcus aeolicus***	**23**	**2–20**	**489**
emg00014	**Hypothetical protein**	***Sulfurihydrogenibium azorense***	**51**	**0.032**	**63**
emg00015	**Conserved hypothetical protein**	***Aspergillus flavus***	**47**	**5–04**	**229**
emg00016	**Hypothetical protein**	***Desulfovibrio magneticus***	**39**	**1–15**	**237**
emg00017	**Pyruvate phosphate dikinase**	***Anaplasma marginale***	**23**	**0.003**	**196**
emg00018	**Hypothetical protein**	***Desulfovibrio magneticus***	**39**	**1–73**	**543**
emg00019	**Putative membrane protein**	***Carboxydothermus hydrogenoformans***	**43**	**5–46**	**358**
emg00020	**Hypothetical protein**	***Bacteroides coprocola***	**35**	**0.16**	**383**
emg00021	**NA**	**NA**	**NA**	**N.A.**	**69**
emg00022	**Condensin subunit Smc**	***Methanohalophilus mahii***	**27**	**1.9**	**252**
emg00023	**NA**	**NA**	**NA**	**N.A.**	**46**
emg00024	**Similar to GA14224-PA**	***Tribolium castaneum***	**22**	**0.14**	**146**
emg00025	**LemA protein (*mamQ-I*)**	***Mitsuokella multacida***	**36**	**5–25**	**186**
emg00026	**Magnetosome protein MamE**	**Uncultured bacterium**	**31**	**2–57**	**603**
emg00027	**Magnetosome protein MamI**	**Magnetic vibrio MV-1**	**29**	**0.78**	**62**
emg00028	**TPR Domain containing protein (*mamA*)**	***Tetrahymena thermophila***	**32**	**8–23**	**216**
emg00029	**Hypothetical membrane protein**	***Desulfovibrio magneticus***	**28**	**1–07**	**127**
emg00030	**Magnetosome protein MamB**	**Uncultured bacterium**	**32**	**3–41**	**297**
emg00031	**LemA protein (*mamQ-II*)**	***Campylobacter showae***	**32**	**2–17**	**182**
emg00032	**Hypothetical protein**	***Desulfitobacterium hafniense***	**27**	**7–08**	**227**
emg00033	**Magnetosome protein MamM**	***Magnetospirillum gryphiswaldense***	**35**	**2–44**	**307**
emg00034	**Magnetosome protein MamP**	**Magnetic vibrio MV-1**	**37**	**2–23**	**375**

Results of BlastP analysis of proteins encoded by predicted genes of the 37,160-bp genomic fragment from *Candidatus Magnetobacterium bavaricum* against the NCBI database. Best BlastP hits are shown. Genes of a magnetosome cluster are in boldface type. The genes *egm00025* and egm00031 encode proteins that were found to contain a LemA motive and were annotated as *mamQ*-like. Gene *egm00028* encodes a protein containing a TPR domain and was annotated as *mamA*-like (see text for details). All other genes were annotated according their best BlastP hits. NCBI, National Center for Biotechnology Information.

Table S2. BlastP similarities of putative magnetosome proteins from *Candidatus* Magnetobacterium bavaricum with their homologs from all MTB sequenced thus far

Protein	MSR-1, %	AMB-1, %	MS-1, %	MV-1, %	MC-1, %	RS-1, %
MamP	38	38	39	37	43	40
MamM	35	35	36	32	36	27
MamQ-II	24	21	21	23	22	26
MamB	31	30	30	30	32	34
MamA	24	23	23	26	NA	25
MamI	25	23	23	29	35	35
MamE	40	26	26	36	30	30
MamQ-I	28	27	28	26	NA	36

Local identity values are shown. See Figs. 4 and 5 and Figs. S7 and S8 for analysis involving ClustalW alignments of entire protein sequences. MTB, magnetotactic bacteria.

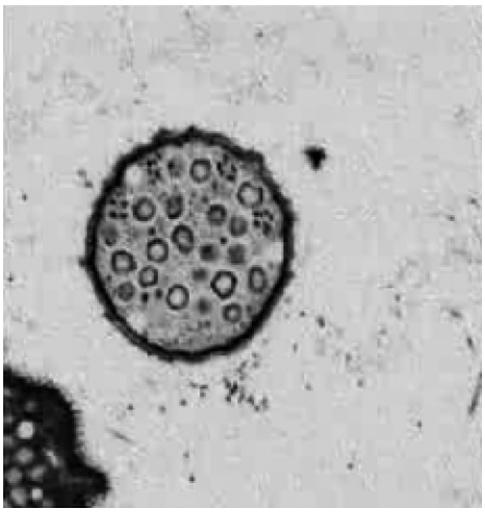

Movie S1. Three-dimensional reconstruction by SEM and focused ion beam (FIB) cross-sectioning (anterior toward posterior) of high-pressure frozen and freeze-substituted *Candidatus* Magnetobacterium bavaricum cell.

Movie S1

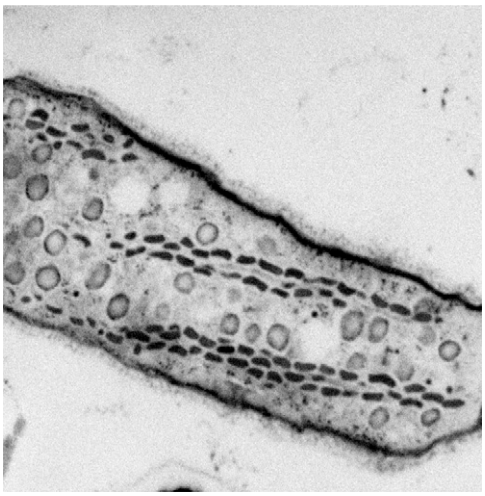

Movie S2. Three-dimensional reconstruction by SEM and FIB tangential sectioning of high-pressure frozen and freeze-substituted *Candidatus* Magnetobacterium bavaricum cell.

Movie S2

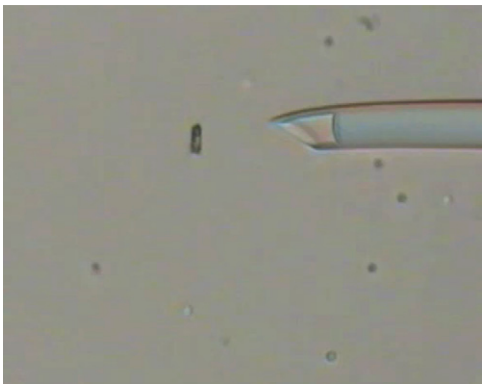

Movie S3. Micromanipulation of *Candidatus* Magnetobacterium bavaricum cells: Selection and aspiration of a single target cell from a mixure of MTB into a microcapillary.

Movie S3

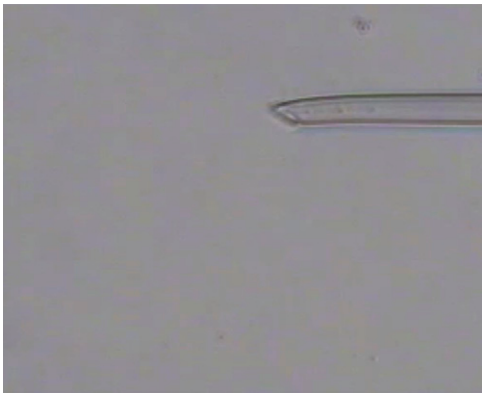

Movie S4. Ejection of >1,000 collected *Candidatus* Magnetobacterium bavaricum cells from a microcapillary into a droplet of pure H_2O. Cells, which had been trapped within the microcapillary for a prolonged time, remained intact and viable in H_2O as indicated by their active swimming motility after release.

Movie S4

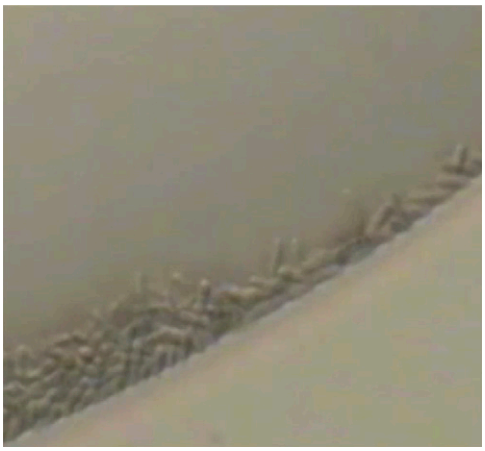

Movie S5. "*Candidatus* Magnetobacterium bavaricum" survives the cell sorting procedure. After being washed and transferred into a droplet of water (Movie S4), cells swim actively toward magnetic north to the edge of the water droplet.

Movie S5